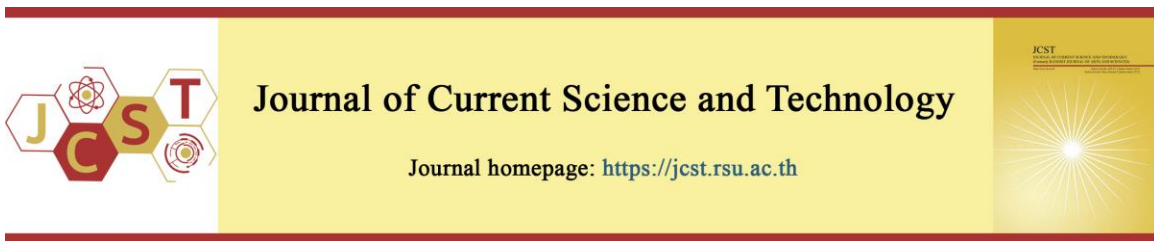


Cite this article: Chitichotpanya, P., Vuthiganond, N., Chutasen, P., & Chitichotpanya, C. (2026). In situ green production of silver nanoparticles utilizing purple corn silk extract for multifunctional healthcare hemp textiles. *Journal of Current Science and Technology*, 16(1), Article 154. <https://doi.org/10.59796/jcst.V16N1.2026.154>



In Situ Green Production of Silver Nanoparticles Utilizing Purple Corn Silk Extract for Multifunctional Healthcare Hemp Textiles

Pisutsaran Chitichotpanya^{1,*}, Nattaya Vuthiganond¹, Pimnara Chutasen², and Chayana Chitichotpanya^{3,4}

¹Department of Materials and Textile Technology, Faculty of Science and Technology, Thammasat University, Pathum Thani 12120, Thailand

²The Newton Sixth Form School, Bangkok 10400, Thailand

³Department of Chemistry, Faculty of Science, Mahidol University, Bangkok 10400, Thailand

⁴Center for Surface Science and Engineering, Faculty of Science, Mahidol University, Nakhon Pathom 73170, Thailand

*Corresponding author; E-mail: pisut_c@tu.ac.th

Received 30 June 2025; Revised 18 August 2025; Accepted 8 September 2025, Published online 20 December 2025

Abstract

This study aimed to create multifunctional healthcare hemp fabrics employing a facile and cost-effective method. Multifunctional hemp was manufactured through in situ green synthesis of silver nanoparticles (AgNPs) employing an anthocyanin extract as both a reducing agent and functional colorant, due to the numerous health benefits linked to anthocyanins derived from purple corn silk (PCS), an agricultural byproduct. XRD and SEM-EDS analyses confirmed AgNP formation and uniform distribution on hemp fibers. The results demonstrated that dyebath pH significantly affected the perceived color, color strength (K/S), UV protection, and antioxidant and antibacterial activities. In an alkaline dyebath, more AgNPs were produced, improving K/S values, UV protection (UPF rating of 50+), and antibacterial efficiency against *S. aureus* and *E. coli*, with *E. coli* exhibiting better efficacy. However, an increase in AgNPs reduced the antioxidant capabilities of the treated fabrics. Overall, this study successfully demonstrated an economical and straightforward method for finishing hemp fabrics for multifunction healthcare textiles. PCS also contains a higher concentration of anthocyanins compared to other natural sources, rendering it an economical anthocyanin resource for textile businesses.

Keywords: purple corn silk; anthocyanin; silver nanoparticle; hemp; antioxidant activity; UV-protection; antibacterial activity

1. Introduction

The healthcare textile market has experienced substantial growth in the last few years, driven by modern consumers' concern for well-being and hygiene (Tat et al., 2022; Libanori et al., 2022). Potential business sectors encompass medical and healthcare goods, household items, sportswear, undergarments, etc. Cotton prevails in the natural cellulose textile sector due to its fluffy texture, thermal insulation, and notable

hygroscopic properties (El Bourakadi et al., 2024). Nevertheless, the climates in the Southeast Asian countries are not appropriate for its economic cultivation. Cannabis sativa, known as hemp, has been adopted as an economic commodity in Southeast Asian countries due to its ecological benefits (Schumacher et al., 2020). The constituents of hemp fiber are: 61% cellulose, 24% hemicellulose, 10% lignin, and 3% extractives (Rehman et al., 2021; Sasunthon et al., 2025).

Nonetheless, a significant disadvantage of cellulose fabrics is their propensity to harbor bacteria, resulting in unpleasant odors, skin infections, allergies, and other associated ailments, as well as low UV protection (Gao et al., 2020; Rehan et al. 2020). Although hemp fibers contain antibacterial agents such as tetrahydrocannabinol, they are still susceptible to microbial attacks (Li et al., 2024). Consequently, the utilization of antimicrobial finishes on hemp fibers is an intriguing area of investigation. Previous studies indicate that the use of nanoparticles, including noble metal and metal oxide nanoparticles, quaternary ammonium compounds, and natural extracts, is effective as biocides in the antimicrobial textile finishes (Gulati et al., 2022; Chang et al., 2021).

Silver (Ag) has been utilized in numerous medical applications since antiquity (Burduşel et al., 2018). The antibacterial efficacy is attributed to the dissociation of silver salts upon contact with water or the diffusion of Ag^+ ions from silver nanoparticles (AgNPs) by oxidation in the presence of water and oxygen (Srisod et al., 2018). AgNPs or Ag^+ ions smaller than 10 nm have been shown to infiltrate microbial cells, disrupting vital physiological functions by modifying metabolic processes and subsequently inhibiting microbial proliferation (Ahmed & Ogulata, 2021; Sasunthon et al., 2025). Silver may expedite the creation of reactive oxygen species (ROS) in the presence of oxygen, which are harmful to microbial organisms (Simončič & Klemenčič, 2016). Coating textiles with silver salts, such as silver chloride (AgCl) or silver nitrate (AgNO_3), causes an uncontrolled reduction process that stains the cloth black-gray when exposed to air and light. Therefore, it is recommended to use more steady AgNPs for applications in the textile field (Ahmed & Ogulata, 2021). AgNPs, nanoscale aggregates of silver metal atoms, exhibit remarkable antimicrobial efficacy because they have a high surface area relative to their size. Consequently, they emit silver ions much easier than bulk silver. AgNPs exhibited biocidal effectiveness at markedly lower concentrations than silver ions (Srisod et al., 2018) and displayed substantial antibacterial activity against diverse bacterial species (Burduşel, 2018). The synthesis of AgNPs can be accomplished via a range of methodologies, encompassing physical, chemical, photochemical, and biological reduction techniques (Huq et al., 2022). The predominant and conventional method for synthesizing AgNPs

involves a chemical reduction of silver salts in an aqueous medium, employing hazardous reducing agents, including hydrazine hydrate, sodium borohydride, or aldehyde compounds. These nanoparticles can then be applied for textile treatment using various techniques, including dip coating, padding, and sol-gel coatings (Ahmed & Ogulata, 2021). There is a trend towards utilizing less toxic and more environmentally sustainable reducing agents, such as plant extracts, polysaccharides, microorganisms, and enzymes. Plant extracts offer a broader range of material sources and are more cost-effective than alternative biological reducing agents. The utilization of microorganisms, however, necessitates additional time owing to the culturing process and the difficulties related to preserving cell structures (Annamalai et al., 2021). Consequently, the utilization of bioactive and biochemical compounds derived from plant-based extracts for the production of AgNPs in biomedical fields has garnered increasing scientific interest (Dhaka et al., 2023). Recent examples of bio-reductions for synthesizing AgNPs include the use of extracts from Black rice, Butterfly pea, Tansy, Indian gooseberry, red cabbage, and purple potato (Čuk et al. 2021; Jain et al., 2022; Velmurugan et al., 2017; Yu et al., 2020; Yu et al., 2021). An aqueous extract from black rice, which contains anthocyanins, has been utilized for concurrent dyeing and synthesis of AgNPs on cotton fabrics (Yu et al., 2020; Yu et al., 2021). These bioactive substances are abundant in phytochemicals, including flavonoids, phenols, terpenoids, and tannins, serving as reducing and stabilizing agents in the synthesis of NPs. Recently, there has been a significant trend towards the use of agricultural byproducts for the synthesis of AgNPs, presenting a more sustainable alternative to plant extracts (Abdallah et al., 2024). This trend highlights an increasing interest in reusing agricultural waste materials to reduce their negative environmental effects. The utilization of agricultural byproducts in nanoparticle synthesis has garnered interest from researchers (Suhag et al., 2022; Vasyliev & Vorobyova, 2020). Research studies have shown that various agricultural byproduct materials, such as fruit peels, oil cakes, and crop straws, can facilitate the formation of AgNPs (Čuk et al., 2021; Ijaz et al., 2020; Monika et al., 2022). These agricultural byproducts contain biomolecules capable of reducing Ag^+ to $\text{Ag}0$. The utilization of agricultural byproducts for the synthesis of bio-based nanoparticles, in accordance with

biorefinery principles, is gaining traction due to its environmentally friendly and non-toxic characteristics, along with its role in promoting resource sustainability (Koul et al., 2022).

Anthocyanins are naturally occurring colored substances present in plant sources. Their role in NP synthesis, especially for silver and gold NPs, has recently gained considerable attention due to their ability to act as reducing and stabilizing agents (Khadem & Kharaziha, 2022; Maneewattanapinyo et al., 2023). The reduction process involves transferring electrons from anthocyanins to metal ions, which facilitates the creation of steady NPs with controlled shapes and sizes. Anthocyanins provide numerous benefits compared to traditional chemical reducing agents, such as non-toxicity, biocompatibility, and sustainability (Neciosup-Puican et al., 2024). Anthocyanins are also the most often used water-soluble natural colorants due to their bright colors, which range from violet, blue, pink, and red depending on pH. Numerous studies indicate that anthocyanins function as potent antioxidants, exhibit antimicrobial properties, and provide protection against ultraviolet radiation (UVR) (Le et al., 2019; Rehan et al., 2022; Sadeghi-Kiakhani et al., 2021). Purple corn, scientifically known as *Zea mays L.*, originating in Peru, has been disseminated worldwide due to its superior health benefits and nutritional values (Kim et al., 2023). Purple corn's high anthocyanin and phenolic content contribute to its outstanding health benefits. Purple corn possesses an enormous number of anthocyanins, especially in the cob, husk, or purple corn silk (PCS), with cyanidin-3-glucoside being its primary anthocyanin component. Figure 1 illustrates that cyanidin-3-glucoside is regarded as a polyphenolic compound, characterized by a large number of hydroxyl groups. These functional groups possess specific reduction properties. Consequently, the anthocyanin extract from purple corn can serve as a reducing and stabilizing agent for AgNP biosynthesis. The husk, cob, and silk of purple corn are considered agricultural waste and have been eliminated after consumption. Corn cobs, husks, and PCS have predominantly been employed for animal feed, charcoal production, and fertilization. Nevertheless, PCS presents potential as an active ingredient in creating health-oriented products, such as tea, herbal remedies, and cosmetics.

Subsequent to our prior study (Klaykruayat et al., 2024), which established the optimal conditions for

ultrasound-assisted anthocyanin extraction from PCS for multifunctional hemp finishes, the current study aimed to investigate the feasibility of PCS extract functioning as a bio-reducing agent for in situ AgNP synthesis across different pH levels to enhance antibacterial properties while simultaneously dyeing hemp fabrics. Moreover, anthocyanins derived from PCS can serve as a multifunctional colorant for hemp finishes, owing to the myriad health benefits linked to anthocyanins. As a result, the hemp fabric was treated with anthocyanin extract, while AgNPs were concurrently deposited onto the hemp fiber's surface in a single bath. The performance evaluations, encompassing color strength, UV protection, antioxidant activity, and antibacterial properties, were also assessed according to standard testing protocols. To our knowledge, there has been no research study on the in situ green synthesis of AgNPs on hemp fibers using PCS extract as both a bio-reducing and stabilizing agent.

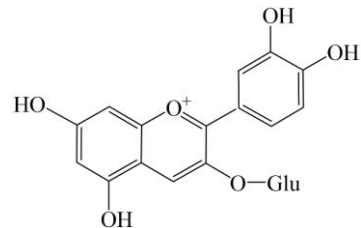


Figure 1 Chemical structure of cyanidin-3-glucoside, the primary anthocyanin component in purple corn silk

2. Objectives

This study examined the feasibility of utilizing agricultural waste, particularly PCS, as a bio-reducing agent for in situ synthesis of AgNPs at various pH levels. Moreover, anthocyanins derived from PCS can serve as a multifunctional colorant for hemp finishes, attributed to their various health benefits. As a result, the hemp fabric was finished with anthocyanin extract, while AgNPs were concurrently deposited on the hemp fiber's surface in a single bath, yielding multifunctional healthcare hemp textiles. The main contributions of our study are: (1) to advocate for the utilization of agricultural byproducts in textile dyeing through a green and nanotechnology approach; (2) to create a cost-effective and straightforward method for manufacturing multifunctional hemp fabrics with enhanced antibacterial properties; and (3) to increase the value of hemp fiber, a commodity fiber in northern Thailand, into textiles with medicinal and healthcare benefits.

3. Materials and Methods

3.1 Materials

A plain woven hemp fabric with a density of 270 g/m², comprising 35 yarns per inch in the warp and 27 yarns per inch in the weft, was sourced from Chiang Mai province, Thailand. PCS was obtained from Sangthong Farm in Phetchabun Province, Thailand. A scouring operation was conducted to remove contaminants from the fabric, utilizing a nonionic detergent (Triton X100) at a concentration of 2 g/L, maintained for 30 min at 70 °C. Silver nitrate (AgNO₃, 99.8% purity) used as the silver precursor was obtained from Sigma-Aldrich (Germany). Glacial acetic acid (CH₃COOH, AR grade) and sodium hydroxide (NaOH, AR grade) were acquired from Ajax Finechem (Australia).

3.2 Methods

3.2.1 Aqueous Anthocyanin Extraction from PCS

After thorough cleaning, PCS was oven-dried for 45 min at 60 °C before being sliced into smaller pieces. Ultrasound-assisted aqueous extraction was employed to extract anthocyanins from PCS through a 3-Liter ultrasonic bath with 35 kHz (Sonorex DIGITEC DT 102 H-RC). The material-to-liquor ratio was 1:10, the temperature was maintained at 65 °C, and the extraction duration was set to 30 minutes (Figure 2). The extracted solutions were subsequently filtered through Whatman No. 1 paper. A pH differential technique (Yin et al., 2017) was employed to evaluate the total anthocyanin content (TAC) of the extracts through absorbance measurements at pH 1.0 and 4.5, facilitating the identification of chemical structural changes in anthocyanin. Two separate standard buffer solutions were prepared. The pH 1.0 solution was prepared by combining 25 mL of 0.2 mol/L potassium chloride with 67 mL of 0.2 mol/L hydrochloric acid. The pH 4.5 solution was formulated by mixing 6 mL of 1 mol/L hydrochloric acid, 10 mL of 1 mol/L sodium acetate,

and 9 mL of DI water. In accordance with equation (1), the TAC was defined and expressed with regard to the cyanidin 3-glucoside equivalent.

$$\text{TAC (mg/l)} = \frac{A \times M_w \times DF \times 1000}{E \times L} \quad (1)$$

Where A represents the absorbance value calculated as $[(A_{\lambda_{\text{max}}} - A_{700})_{\text{pH}1.0} - (A_{\lambda_{\text{max}}} - A_{700})_{\text{pH}4.5}]$. Cyanidin 3-glucoside has a molecular weight of 449.2 g/mol and a molar extinction coefficient (E) of 26,900. DF denotes the dilution factor, while L refers to the cuvette's path length.

3.2.2 Simultaneously dyeing and *in situ* synthesis of AgNPs using anthocyanin extract

AgNPs were *in situ* synthesized following the methodologies outlined by Balamurugan et al. (2017) and Yu et al. (2020), as shown in Figure 3. First, a scoured hemp sample (5 cm x 10 cm) was immersed for 30 minutes in 100 mL of 20 mmol/L AgNO₃ solution at room temperature. The hemp sample was subsequently processed with a padding machine (Labtec, Newave Lab Equipments Co. Ltd., Taiwan) to obtain a wet pick-up of 80%. The wet padding sample was then oven-dried at 80 °C for 20 min. An exhaust method with a material-to-liquor ratio of 1:20 was employed to dye the padded hemp sample with anthocyanin extract solution, utilizing an infrared dyeing machine (Starlet DL-6000, Daelim Starlet Co. Ltd., South Korea) for 60 min at 65 °C. The dyebath pH was adjusted to 4, 7, and 10 using acetic acid and sodium hydroxide. In order to ensure the anthocyanin's structural stability, the dyeing temperature was established at 65 °C (Yu et al., 2020). Finally, the hemp samples were thoroughly rinsed with DI water to eliminate excess colorants and then air-dried.



Figure 2 Ultrasound-assisted aqueous extraction from PCS

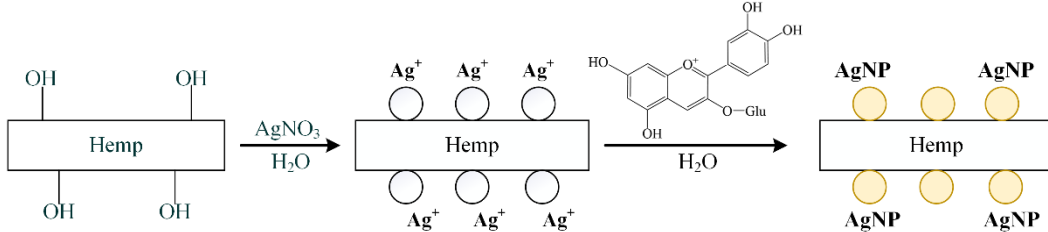


Figure 3 Schematic diagram of anthocyanin dyeing and in situ AgNP deposition on hemp fabrics

3.2.3 Evaluation of Fabric Morphology

Examining the morphology of the AgNP-treated fabric is essential to analyze the distribution of nanoparticles on the hemp fibers. The crystallinity of the fabric treated with AgNP was examined using X-ray diffraction (XRD, Bruker D8 advanced Diffractometer, Bruker Corporation, Germany) with a Cu anode ($\lambda = 0.154$ nm) at 40 keV, 6 °C/min, and scanned from 10° to 80° (2 Θ). The morphology of the treated fabric was further analyzed utilizing the field emission scanning electron microscope (FE-SEM, JEOL JSM7800F, Japan) with an accelerating voltage of 2.0 kV and a magnification of 5,000x. Before conducting the observation, a thin gold film was applied to all samples through sputter coating. Elemental mapping via SEM-EDS was conducted utilizing a microscope (JEOL, JSM-IT700HR, Japan). The accelerating voltage was established at 5.0 kV, accompanied by a magnification of 800x.

3.2.4 Color Measurement

The colorimetric coordinates of the treated hemp samples were determined using a spectrophotometer (GretagMacbeth Color i5, USA). The spectrophotometer included an illuminant D65 with a 10° standard observer, including specular and UV components. Each test was conducted three times, with the average score documented. The color strength (K/S) was calculated using the Kubelka-Munk equation (Eq. 2).

$$\frac{K}{S} = \frac{(1-R)^2}{2R} \quad (2)$$

Where R, K, and S denote the reflectance at the peak absorption wavelength, the absorption coefficient, and the scattering coefficient, respectively.

The colorimetric coordinates are represented by CIELAB color space (L^* , a^* , b^* , h° , and C^*). L^* represents brightness, where 0 signifies black and 100

signifies white. The red-green axis is represented by a^* , where positive values denote red and negative ones denote green. The b^* denotes the blue-yellow axis, where negative values indicate blue and positive values indicate yellow. C^* denotes chroma, while h° signifies hue angle.

3.2.5 Assessment of UV Protection

The UVR transmittance and Ultraviolet protection factor (UPF) of fabric samples were determined through a double-beam CamSpec M550 SPF Spectrophotometer (Spectronic CamSpec Ltd., UK) in accordance with AATCC TM183-2000 (Table 1) (Sasunthon et al., 2025). The percent transmittance quantifies the amount of UVR exposure to the skin, whereas UPF value is the rating index that evaluates a fabric's effectiveness in protecting against UVR. A higher UPF value suggests that fabrics are more effective at blocking UVR (Banupriya & Priyanka, 2018). The UPF values are calculated using Equation (3). Equations (4) and (5) represent the average transmittance values in the UV-A range (315-400 nm) and UV-B range (290-315 nm), respectively. All results were obtained from the average of three replicates.

$$UPF = \frac{\sum_{290 \text{ nm}}^{400 \text{ nm}} R_\lambda S_\lambda \Delta\lambda}{\sum_{290 \text{ nm}}^{400 \text{ nm}} R_\lambda S_\lambda T_\lambda \Delta\lambda} \quad (3)$$

$$T(\text{UVA}) = \frac{\sum_{315 \text{ nm}}^{400 \text{ nm}} T_\lambda \Delta\lambda}{\sum_{315 \text{ nm}}^{400 \text{ nm}} \Delta\lambda} \quad (4)$$

$$T(\text{UVB}) = \frac{\sum_{290 \text{ nm}}^{315 \text{ nm}} T_\lambda \Delta\lambda}{\sum_{290 \text{ nm}}^{315 \text{ nm}} \Delta\lambda} \quad (5)$$

Where R_λ , S_λ , $\Delta\lambda$, and T_λ denote the relative erythema spectrum effectiveness, the solar spectrum irradiance, the wavelength interval (nm), and the average spectrum transmittance, respectively.

3.2.6 Assessment of Antioxidant and Antibacterial Activities

The antioxidant efficacy of treated hemp samples was evaluated through the DPPH (2, 2-Diphenyl-1-picrylhydrazyl) radical scavenging technique (Sadeghi-Kiakhani et al., 2021). A 500 mg fabric sample was submerged in 50 mL of 0.20 mM DPPH methanol solution and incubated in the darkness for 20 minutes. The solution exhibited a color change from deep purple to light yellow, with its absorbance at 518 nm was quantified using a UV spectrometer. Ascorbic acid served as a positive control. The antioxidant activity percentage was determined using Equation (7).

$$\text{Antioxidant activity (\%)} = \frac{U - T}{U} \times 100 \quad (7)$$

Where U and T represent the absorption values at 518 nm for untreated and treated fabric samples, respectively, in dark-incubated solutions.

The antibacterial efficacy of treated hemp samples was evaluated qualitatively using the Parallel streak method (AATCC TM147-2019) against *S. aureus* (ATCC 6538, gram-positive) and *E. coli* (ATCC 25922, gram-negative). The zone of inhibition, which is an area free of bacteria at the edge of the test specimen, was calculated using Equation (8).

$$\text{Zone of inhibition (mm)} = \frac{T - D}{2} \quad (8)$$

Where T and D represent the total diameter of the test specimen plus the zone of inhibition (mm) and the diameter of the test specimen (mm), respectively.

3.2.7 Statistical Analysis

The TAC of the PCS extract, color strength, colorimetric values, UV protection, and antioxidant properties were each measured in triplicate, and the net averages were documented and analyzed.

4. Results and Discussion

4.1 TAC of PCS Extract

The TAC of the PCS extract was assessed via the pH differential method. Figure 4 illustrates the spectra of anthocyanin extract from PCS in buffers at pH 1.0 and 4.5, indicating that the greatest absorption occurred at 508 nm. The total content of isolated anthocyanins, as determined by equation (1), was 571.25 mg/100 g of PCS. PCS appears to possess a high anthocyanin concentration relative to other natural anthocyanin sources, such as purple potato (Neciosup-Puican et al., 2024) and black rice bran (Klaykruayat et al., 2025).

Table 1 Classification of UVR protection efficiency according to AATCC TM183-2000

UVR transmittance (%)	UVR blocking (%)	UPF	UVR protection efficiency
Less than 2.5	More than 97.5	40 – 50+	Excellent
4.1 – 2.6	96.0 – 97.4	25 – 39	Very Good
6.7 – 4.2	93.3 – 95.9	15 – 24	Good

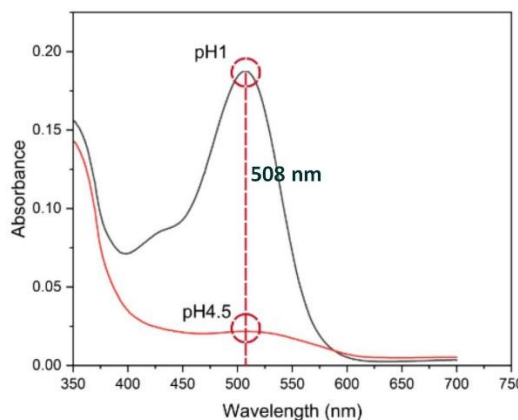


Figure 4 UV-visible absorption spectra of PCS extract at pH 1.0 and pH 4.5 for total anthocyanin content determination

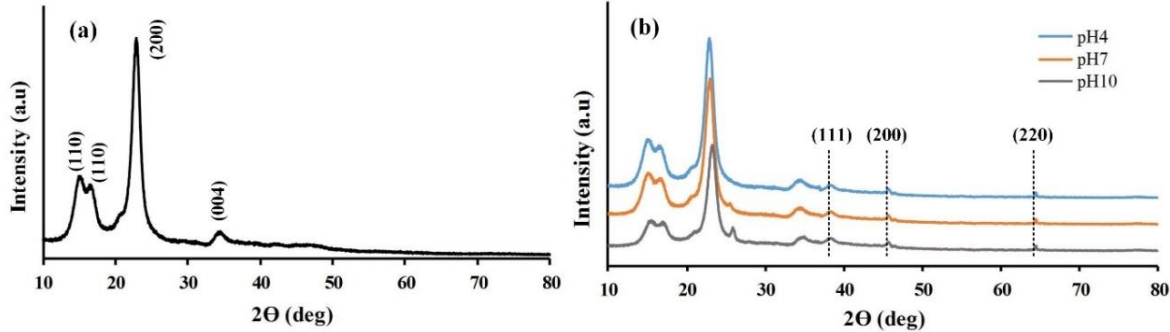


Figure 5 XRD patterns of (a) untreated hemp and (b) treated hemp at various pH values

4.2 In-situ Synthesis of AgNPs on Hemp Fabric

The XRD technique was employed to ascertain the production of AgNPs deposited *in situ* on dyed hemp fibers at different pH levels and to examine their crystal structure. Figure 5 illustrates the XRD patterns of both untreated hemp sample and treated hemp samples at pH values of 4, 7, and 10. All samples have pronounced diffraction peaks at 2Θ values of 15° , 16.5° , 23.2° , and 34.2° , which correspond to the (110), (110), (200), and (004) planes of standard cellulose diffractions, respectively (Balamurugan et al., 2017). In contrast to the untreated hemp fabric (Figure 5(a)), three extra peaks appear at 2Θ values of 38.2° , 45.1° , and 65° (Figure 5(b)) for all treated hemp samples at different pH levels. These correspond to the (111), (200), and (220) planes of AgNPs. This confirms that AgNPs were effectively produced and deposited on all hemp samples at various pH values. Nevertheless, it is observed that the AgNP-loaded hemp samples do not show a strong peak of AgNP, attributed to the small amount of elemental silver in the treated hemp samples.

SEM images further confirmed the successful synthesis of AgNPs on treated hemp fabrics. The surface morphology of treated hemp samples at various pH levels is shown in Figure 6. The untreated hemp fabric

showed a smooth surface (Figure 6(a)). In contrast, treated hemp surfaces at different pH levels showed some roughness attributable to an adherence of *in situ* AgNPs (Figure 6(b-d)), especially at pH values of 10. However, AgNPs were distributed evenly on the surface of treated hemp samples, ensuring that the hemp samples containing AgNPs had consistent color and antibacterial properties. The elemental composition of AgNPs deposited on hemp fabric samples was further analyzed based on the SEM-EDS spectrum, as shown in Figure 7. It provided a semi-quantitative indication of the weight percentages of silver in the hemp samples. As shown in Figure 7(a), no elemental silver was detected in the untreated hemp sample. The treated hemp samples exhibited a distinct Ag signal near 3 keV, indicating the AgNP formation on the surface of the hemp samples (Figure 7(b-d)). The Ag content increased from 1.1 to 3.2 wt% for samples synthesized at pH levels ranging from pH 4 to pH 10, with the maximum content observed at pH 10. The AgNP content should be adequate for the release of silver ions to attain effective antibacterial efficacy. Ultimately, the SEM and SEM-EDS results confirmed the feasibility of producing antibacterial textiles through this eco-friendly method.

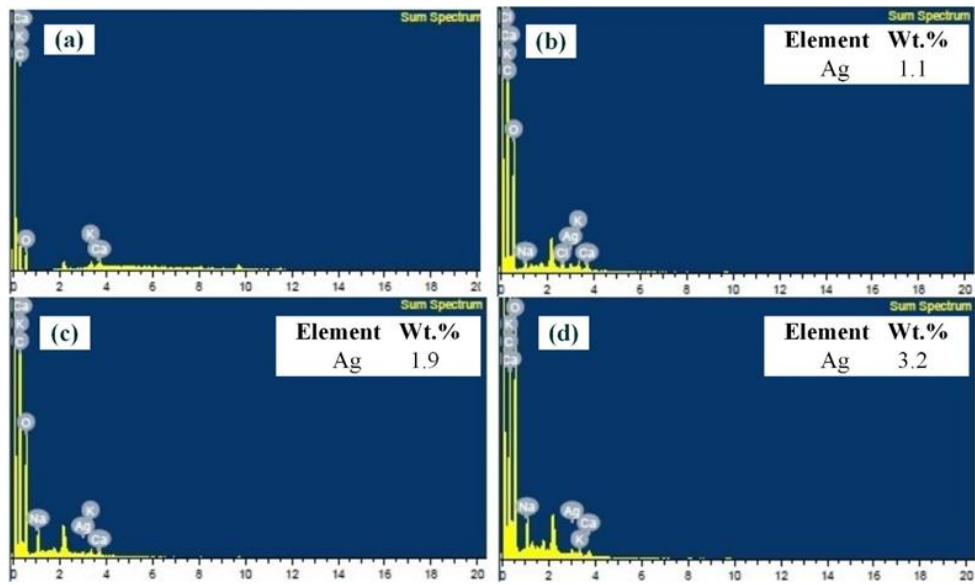


Figure 6 SEM images at 5000x: (a) untreated and (b) treated at pH 4, (c) pH 7, and (d) pH 10

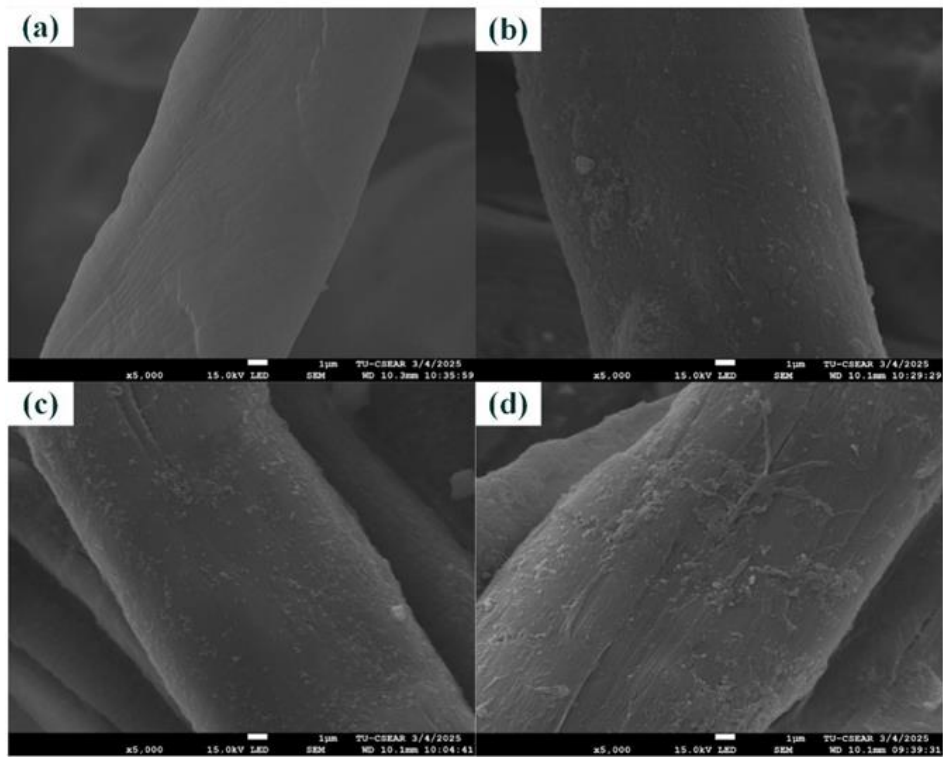


Figure 7 SEM-EDS images: (a) untreated and (b) treated at pH 4, (c) pH 7, and (d) pH 10

Table 2 Color strength (K/S) and colorimetric values of hemp fabrics treated at different pH levels.

Hemp samples	CIE values					K/S	Image
	<i>L</i> *	<i>a</i> *	<i>b</i> *	<i>C</i> *	<i>h</i> °		
Untreated	89.17	0.22	4.26	4.27	87.07	0.17	
pH 4	59.27	18.44	7.85	16.70	23.06	2.53	
pH 7	57.32	7.39	14.44	13.52	62.90	3.87	
pH 10	49.56	5.26	20.99	18.03	75.93	5.54	

4.3 Evaluation of Colorimetric Parameters

This study evaluated CIELAB colorimetric values and K/S values of treated hemp samples across varying dyebath pH levels. Table 2 demonstrates the treated hemp fabrics displayed different colors at pH levels of 4, 7, and 10. The rationale of this is as follows. First, the quantity of AgNPs that were deposited on the hemp fabric varied depending on the pH level. Consequently, the treated hemp fabrics exhibited different colors at varying pH levels. Secondly, the anthocyanin present in PSC was a contributing factor. At varying pH levels, anthocyanin undergoes a significant transformation in color. The molecular structure transformations of anthocyanins are associated with these color changes in the pH range, which result from protonation and deprotonation reactions caused by pH changes in the dyebath (Khadem & Kharaziha, 2022; Roy & Rhim, 2021). When the dyebath is acidic, anthocyanins exist in the form of molten salt positive ion with red color (Yu et al., 2021). Among these samples, a pronounced yellow hue was observed in the treated hemp fabrics at pH values of 7 and 10, with the pH of 10 exhibiting a significant increase in the *b** value. The yellow hue in treated hemp fabrics indicates the formation and accumulation of AgNPs on the fabric's surface, due to the surface plasmon resonance characteristics of AgNPs (Jiang et al., 2022). However, it was observed that the treated samples did not exhibit a noticeable yellow hue at pH 4. This finding indicates that AgNPs can be readily synthesized in an alkaline reaction solution. Our results are consistent with prior research conducted by (Velmurugan et al., 2017; Yu et al., 2020). The colorimetric values of the treated hemp samples were also defined by K/S values (Table 2). The sequence of treated samples based on K/S values was

pH 4 < pH 7 < pH 10. The K/S value peaked at pH 10, then dropped to a minimum at pH 4. The results also indicated that AgNPs were uniformly distributed on the surface of the hemp samples in an alkaline condition. Therefore, alkaline conditions are required for the synthesis of AgNPs via this method.

4.4 Evaluation of UV Protection and Antioxidant Properties

Appropriate UVR is advantageous to humans as it disinfects and facilitates the synthesis of vitamin D. Nevertheless, elevated levels of UVR may lead to sunburn and potentially skin cancer (Attia et al., 2022). Textiles function as an important barrier between humans and their surroundings, thereby providing UV protection. However, several factors that influence the level of UV protection in textiles. The type of fibers and construction of fabrics substantially influence UV protection, with thicker and denser materials providing superior defense against UVR. Natural fibers typically offer limited UV protection. The dyeing process influences UV protection, with darker colors offering enhanced shielding. Additionally, several natural dyes can absorb both UV and visible light, enabling them to effectively block UV radiation while also imparting color (Chitichotpanya et al., 2024).

This study evaluated the effectiveness of UV protection offered by hemp fabric coated with extracted anthocyanin/AgNP by measuring the percentage of UVR transmitted through the fabric and determining the UPF value. Table 3 compares treated and untreated hemp samples based on UPF values, UV-A and UV-B transmission percentages, and UV-A and UV-B blocking percentages. The results reveal a notable difference between untreated and treated hemp samples.

The untreated hemp fabric possesses a UPF of 13.8. It intrinsically lacks UV-absorbing chemicals and carbon-carbon double bonds in its fiber molecular structure, rendering it incapable of providing sufficient UV protection (Kibria et al., 2022). Hemp samples dyed with anthocyanin, regardless of pH differences, possessed functional groups (polyphenol and flavonoid) that absorb UV radiation, offering excellent UV protection (UPF 50+) to the treated fabrics. This is corroborated by decreased percent transmittance and higher UPF values compared to those of the untreated sample. Hemp samples dyed with anthocyanin, regardless of pH differences, exhibited functional groups such as polyphenol and flavonoid that absorb UVR, offering enhanced UV protection compared to untreated samples. Furthermore, the increased UV protection in treated hemp samples is due to the surface plasmon resonance absorption properties of AgNPs to obstruct UV penetration (Rajaboopathi & Thambidurai, 2018). The hemp sample treated at pH 10 exhibited the highest UPF value and the lowest UV-A and UV-B transmission among the samples, attributable to a greater concentration of AgNPs under alkaline

conditions. The findings align with the research studies conducted by (Barani & Mahltig, 2020; Yu et al., 2020).

The integration of antioxidants into textiles that come into direct contact with the skin sparks significant interest in the development of health-enhancing clothing. Research works have demonstrated the efficacy of anthocyanin toward radical scavenging, suggesting it could be a natural antioxidant to augment the textile's antioxidant properties (Klaykruayat et al., 2024; Klaykruayat et al., 2025). Therefore, this study evaluated the antioxidant activity of hemp samples treated with anthocyanin/AgNP, utilizing the DPPH assay as shown in Figure 8. The treated hemp sample demonstrated the highest antioxidant activity at 84.4%. This may be attributed to the anthocyanin extract's radical-scavenging capacity, owing to the presence of active hydrogen groups in polyphenolic compounds (Kumar et al., 2021; Rehan et al., 2022). However, the treated hemp at pH 10 demonstrated lower antioxidant activity than the other samples because of an increased content of AgNPs in alkaline conditions, which reduced free hydroxyl groups through interactions among hemp, metal ions, and dye molecules (Rehan et al., 2020).

Table 3 UPF values and UV protection classification of treated hemp fabrics (AATCC TM183-2000)

Sample	Transmittance (%)		Blocking (%)		UPF rating	UPF protection class
	UV-A	UV-B	UV-A	UV-B		
Untreated	15.1	9.26	84.9	90.74	13.8	No class
pH4	2.8	2.5	97.2	97.5	50+	Excellent
pH7	2.3	2.0	97.7	98	50+	Excellent
pH10	1.8	1.5	98.2	98.5	50+	Excellent

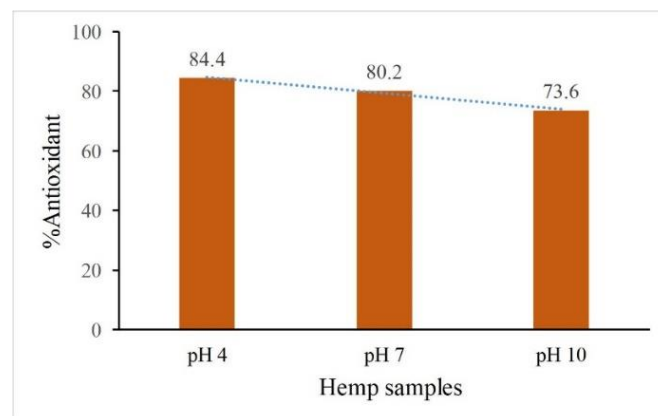


Figure 8 Antioxidant activity of the treated hemp fabrics at various pH levels

4.5 Evaluation of Antibacterial Activity

Hemp fibers inherently possess antibacterial capabilities owing to the presence of bactericidal substances, such as alkaloids, cannabinoids, lignin, and other bioactive compounds (Khan, 2014). Nonetheless, these bactericidal agents are frequently eliminated during the degumming process, resulting in a reduction of the antibacterial efficacy of hemp textiles. Therefore, this study employed the qualitative parallel streak method following AATCC TM147-2019 to assess the antibacterial efficacy of untreated and treated hemp fabrics against *S. aureus* and *E. coli*, measured by the zone of inhibition. No inhibition zone was detected surrounding the untreated hemp sample, whereas the treated samples exhibited a pronounced inhibition zone (Figure 9). The results demonstrate that all treated samples display antibacterial activity against both *S. aureus* and *E. coli*, with *E. coli* being more affected by the in-situ green AgNP synthesis at various pH levels. The hemp sample treated at pH 10 showed the strongest antibacterial effect, with 1.4 mm inhibition zones for *S. aureus* and 1.8 mm for *E. coli*, compared to samples treated at other pH levels. The hemp sample treated at pH 7 and 4 exhibited inhibition zones of 1.1 mm and 0.9 mm for *S. aureus*, and 1.5 mm and 1.2 mm for *E. coli*, respectively. Nevertheless, all the treated samples exhibited a small zone of inhibition due to the insoluble nature of AgNPs. A small amount of Ag⁺ ions was released from AgNPs in a humid environment within the treated samples. The inhibition zone surrounding the treated samples was rather restricted. Our findings suggest that the antibacterial effectiveness of treated hemp textiles is pH-dependent due to increased AgNP

content in alkaline conditions and the specific type of bacteria. Our findings are aligned with previous studies by Velmurugan et al. (2017) and Yu et al. (2020). Although AgNPs offer antimicrobial advantages in healthcare textiles, their cytotoxicity raises significant concerns, particularly due to the release of silver ions and reactive oxygen species (ROS) that may harm mammalian cells (Liao et al., 2019). The cytotoxicity of AgNPs in mammalian cells is significantly influenced by factors such as particle size, shape, dosage, time, surface charge, oxidation state, agglomeration conditions, and the specific cell type involved (Noga et al., 2023). Nonetheless, AgNPs can exhibit no cytotoxicity to mammalian cells while demonstrating significant antibacterial efficacy in specific instances (Sánchez et al., 2016; Srisod et al., 2018). The cytotoxicity of AgNPs can be mitigated through the green formation of AgNPs (Jaswal & Gupta, 2023). AgNPs stabilized with suitable bio-based polymers at specific concentrations also demonstrate no cytotoxicity (Nie et al., 2023). Chitichotpanya et al. (2024) showed that sericin-capped AgNPs exhibited antibacterial activity against *E. coli*, and *S. aureus*, and they did not exhibit cytotoxic effects on mammalian cells (L929 cell line) at the bactericidal concentration (Chitichotpanya & Chitichotpanya, 2017). Overall, while AgNPs provide antimicrobial benefits in textiles, their potential cytotoxicity should be carefully considered. Understanding the variables that influence their toxicity and the mechanisms by which they cause cellular damage is critical to ensuring the safe and sustainable utilization of AgNPs in healthcare or medical textiles.

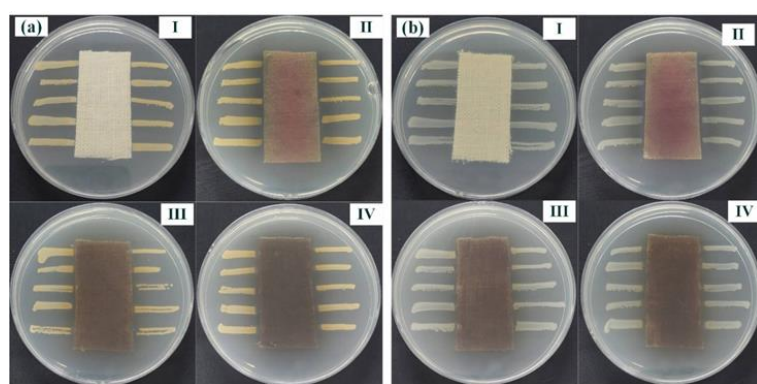


Figure 9 Antibacterial efficacy against (a) *S. aureus* and (b) *E. coli*, with I, II, III, and IV showing untreated, treated at pH 4, pH 7, and pH 10 of hemp samples, respectively.

5. Conclusion

This study shows that multifunctional hemp textiles can be fabricated via green synthesis of AgNPs using an anthocyanin extract from agricultural waste PCS as both a reducing agent and a functional colorant, due to the numerous health benefits linked to anthocyanin. Initially, anthocyanins from PCS were extracted through ultrasonic-assisted aqueous extraction at a frequency of 35 kHz, a temperature of 65 °C, and a duration of 30 min, yielding a TAC of 571.25 mg/100 g of PCS. PCS has much more anthocyanins than other natural sources, making it an attractive new resource for anthocyanins in the textile sector. In the next phase, multifunctional hemp fabrics were successfully produced by concurrently dyeing and in situ synthesizing AgNPs onto hemp fabrics under various pH levels. The formation of AgNP was confirmed through XRD and SEM-EDS analyses, demonstrating a uniform distribution on the hemp fiber surface. Our results illustrate that the synthesis bath's pH levels greatly affect the hue, color strength, UV protection, and antioxidant and antibacterial activities of treated hemp fabrics. The treated samples exhibited a yellowish color due to the presence of AgNPs. The variations in hue and color strength affected by the dyebath pH resulted from the differing quantities of AgNP applied to the fabric and the sensitivity of the anthocyanin extract to pH levels. Anthocyanin extract and AgNPs provided excellent UV protection to the treated hemp fabrics, achieving a UPF value exceeding 50 for all samples. The treated hemp sample demonstrated the peak antioxidant activity of 84.4% at pH 4, subsequently decreasing under alkaline conditions in the dyebath, which reduced the availability of free hydroxyl groups due to interactions among hemp, metal ions, and dye molecules. The inhibition zone indicated that the treated hemp fabrics demonstrated excellent antibacterial activities against *S. aureus* and *E. coli*, particularly under alkaline conditions, with the latter displaying a stronger effect. However, the formation of AgNPs on treated hemp fabrics led to reduced antioxidant properties. Overall, this study demonstrates a cost-effective and straightforward method for producing multifunctional healthcare hemp fabrics via in situ green synthesis of AgNPs using PCS extract.

6. Abbreviations

Abbreviation	Full Term
AgNPs	silver nanoparticles
FE-SEM	field emission scanning electron microscope
K/S	color strength
PCS	purple corn silk
SEM-EDS	scanning electron microscopy coupled with energy dispersive spectroscopy
TAC	total anthocyanin content
UPF	ultraviolet protection factor
UV-A	ultraviolet A
UV-B	ultraviolet B
UVR	ultraviolet radiation
XRD	x-ray diffraction

7. CRediT Statement

Pisutsaran Chitichotpanya: Conceptualization, Methodology, Formal Analysis, Writing – Original Draft, Supervision, Funding Acquisition.
Nattaya Vuthiganond: Investigation, Resources, Validation, Data Curation, Formal Analysis.
Pimnara Chutases: Laboratory Experiments, Visualization, Statistical Analysis.
Chayanisa Chitichotpanya: Conceptualization, Methodology, Resources, Writing – Review & Editing.

8. Acknowledgements

This study was supported by Thammasat University Research Fund, Contract No. TUFT 014/2568.

9. References

Abdallah, S. E., Elmessery, W. M., Elfallawi, F. E., & Shoueir, K. R. (2024). Utilizing agricultural biowaste for food safety: Integrating naturally synthesized silver nanoparticles as antibacterial coating. *Inorganic Chemistry Communications*, 163, Article 112337.
<https://doi.org/10.1016/j.inoche.2024.112337>

Ahmed, T., & Ogulata, R. T. (2021). A review on silver nanoparticles-green synthesis, antimicrobial action and application in textiles. *Journal of Natural Fibers*, 19(14), 8463-8484.
<https://doi.org/10.1080/15440478.2021.1964135>

Annamalai, J., Ummalyma, S. B., Pandey, A., & Bhaskar, T. (2021). Recent trends in microbial

nanoparticle synthesis and potential application in environmental technology: a comprehensive review. *Environmental Science and Pollution Research*, 28(36), 49362-49382.
<https://doi.org/10.1007/s11356-021-15680-x>

Attia, N. F., Osama, R., Elashery, S. E., Kalam, A., Al-Shehmi, A. G., & Algarni, H. (2022). Recent advances of sustainable textile fabric coatings for UV protection properties. *Coatings*, 12(10), Article 1597.
<https://doi.org/10.3390/coatings12101597>

Balamurugan, M., Saravanan, S., & Soga, T. (2017). Coating of green-synthesized silver nanoparticles on cotton fabric. *Journal of Coatings Technology and Research*, 14(3), 735-745. <https://doi.org/10.1007/s11998-016-9894-1>

Banupriya, J., & Priyanka, A. (2018). Application of ultraviolet protection finish on tencel cotton fabric using carica papaya. *Smartex Fashion*, 18, 141-146.

Barani, H., & Mahltig, B. (2020). Using microwave irradiation to catalyze the in-situ manufacturing of silver nanoparticles on cotton fabric for antibacterial and UV-protective application. *Cellulose*, 27(15), 9105-9121.
<https://doi.org/10.1007/s10570-020-03400-6>

Burduşel, A. C., Gherasim, O., Grumezescu, A. M., Mogoantă, L., Ficai, A., & Andronescu, E. (2018). Biomedical applications of silver nanoparticles: An up-to-date overview. *Nanomaterials*, 8(9), Article 681.
<https://doi.org/10.3390/nano8090681>

Chang, L., Duan, W., Huang, S., Chen, A., Li, J., Tang, H., ... & Li, D. (2021). Improved antibacterial activity of hemp fibre by covalent grafting of quaternary ammonium groups. *Royal Society Open Science*, 8(3), Article 201904.
<https://doi.org/10.1098/rsos.201904>

Chitichotpanya, P., & Chitichotpanya, C. (2017). In vitro assessment of sericin-silver functionalized silk fabrics for enhanced UV protection and antibacterial properties using experimental design. *Coatings*, 7(9), Article 145.
<https://doi.org/10.3390/coatings7090145>

Chitichotpanya, P., Vuthiganond, N., Inprasit, T., & Chutasen, P. (2024). Bioactive and multifunctional wool textiles finishing with diospyros mollis griff. extract. *Journal of Current Science and Technology*, 14(1), Article 3. <https://doi.org/10.59796/jcst.V14N1.2024.3>

Čuk, N., Šala, M., & Gorjanc, M. (2021). Development of antibacterial and UV protective cotton fabrics using plant food waste and alien invasive plant extracts as reducing agents for the in-situ synthesis of silver nanoparticles. *Cellulose*, 28(5), 3215-3233.
<https://doi.org/10.1007/s10570-021-03715-y>

Dhaka, A., Mali, S. C., Sharma, S., & Trivedi, R. (2023). A review on biological synthesis of silver nanoparticles and their potential applications. *Results in Chemistry*, 6, Article 101108.
<https://doi.org/10.1016/j.rechem.2023.101108>

El Bourakadi, K., Semlali, F. Z., Hammi, M., & El Achaby, M. (2024). A review on natural cellulose fiber applications: Empowering industry with sustainable solutions. *International Journal of Biological Macromolecules*, 281(2), Article 135773.
<https://doi.org/10.1016/j.ijbiomac.2024.135773>

Gao, D., Liu, J., Lyu, L., Li, Y., Ma, J., & Baig, W. (2020). Construct the multifunction of cotton fabric by synergism between nano ZnO and Ag. *Fibers and Polymers*, 21(3), 505-512.
<https://doi.org/10.1007/s12221-020-9347-4>

Gulati, R., Sharma, S., & Sharma, R. K. (2022). Antimicrobial textile: recent developments and functional perspective. *Polymer Bulletin*, 79(8), 5747-5771. <https://doi.org/10.1007/s00289-021-03826-3>

Huq, M. A., Ashrafudoulla, M., Rahman, M. M., Balusamy, S. R., & Akter, S. (2022). Green synthesis and potential antibacterial applications of bioactive silver nanoparticles: A review. *Polymers*, 14(4), Article 742.
<https://doi.org/10.3390/polym14040742>

Ijaz, M., Zafar, M., & Iqbal, T. (2020). Green synthesis of silver nanoparticles by using various extracts: A review. *Inorganic and Nano-Metal Chemistry*, 51(5), 744-755.
<https://doi.org/10.1080/24701556.2020.1808680>

Jain, A., Kongham, B., Puttaswamy, H., Butola, B. S., Malik, H. K., & Malik, A. (2022). Development of wash-durable antimicrobial cotton fabrics by in situ green synthesis of silver nanoparticles and investigation of their antimicrobial efficacy

against drug-resistant bacteria. *Antibiotics*, 11(7), Article 864.
<https://doi.org/10.3390/antibiotics11070864>

Jaswal, T., & Gupta, J. (2023). A review on the toxicity of silver nanoparticles on human health. *Materials Today: Proceedings*, 81, 859-863.
<https://doi.org/10.1016/j.matpr.2021.04.266>

Jiang, H., Guo, R., Mia, R., Zhang, H., Lü, S., Yang, F., ... & Liu, H. (2022). Eco-friendly dyeing and finishing of organic cotton fabric using natural dye (gardenia yellow) reduced-stabilized nanosilver: Full factorial design. *Cellulose*, 29(4), 2663-2679.
<https://doi.org/10.1007/s10570-021-04401-9>

Khadem, E., & Kharaziha, M. (2022). Red cabbage anthocyanin-functionalized tannic acid-silver nanoparticles with pH sensitivity and antibacterial properties. *Materials Chemistry and Physics*, 291, Article 126689.
<https://doi.org/10.1016/j.matchemphys.2022.126689>

Khan, B. A., Warner, P., & Wang, H. (2014). Antibacterial properties of hemp and other natural fibre plants: A review. *BioResources*, 9(2), 3642-3659.
<https://doi.org/10.15376/biores.9.2.Khan>

Kibria, G., Repon, M. R., Hossain, M. F., Islam, T., Jalil, M. A., Aljabri, M. D., & Rahman, M. M. (2022). UV-blocking cotton fabric design for comfortable summer wears: Factors, durability and nanomaterials. *Cellulose*, 29(14), 7555-7585. <https://doi.org/10.1007/s10570-022-04710-7>

Kim, H. Y., Lee, K. Y., Kim, M., Hong, M., Deepa, P., & Kim, S. (2023). A review of the biological properties of purple corn (*Zea mays* L.). *Scientia Pharmaceutica*, 91(1), Article 6.
<https://doi.org/10.3390/scipharm91010006>

Klaykruayat, B., Vuthiganond, N., & Chitichotpanya, P. (2024). Optimization of ultrasound-assisted anthocyanin extraction from agricultural waste purple corn silk for multifunctional hemp finishes. *Journal of Metals, Materials and Minerals*, 34(4), 2027-2027.
<https://doi.org/10.55713/jmmm.v34i4.2027>

Klaykruayat, B., Vuthiganond, N., & Chitichotpanya, P. (2025). Optimization of ultrasound-assisted anthocyanin extraction from black rice bran for simultaneous coloring, UV protection, and antioxidant silk finishes. *Journal of Current Science and Technology*, 15(1), Article 86.
<https://doi.org/10.59796/jest.V15N1.2025.86>

Koul, B., Yakoob, M., & Shah, M. P. (2022). Agricultural waste management strategies for environmental sustainability. *Environmental Research*, 206, Article 112285.
<https://doi.org/10.1016/j.envres.2021.112285>

Kumar, K., Srivastav, S., & Sharanagat, V. S. (2021). Ultrasound assisted extraction (UAE) of bioactive compounds from fruit and vegetable processing by-products: A review. *Ultrasonics Sonochemistry*, 70, Article 105325.
<https://doi.org/10.1016/j.ultsonch.2020.105325>

Le, X. T., Huynh, M. T., Pham, T. N., Than, V. T., Toan, T. Q., Bach, L. G., & Trung, N. Q. (2019). Optimization of total anthocyanin content, stability and antioxidant evaluation of the anthocyanin extract from Vietnamese *Carissa carandas* L. fruits. *Processes*, 7(7), Article 468. <https://doi.org/10.3390/pr7070468>

Li, D., & Sun, Y. (2024). Using gardenia pigment for ultrasonic natural dyeing of hemp fiber: A step towards sustainable dyeing. *Industrial Crops and Products*, 222, Article 119528.
<https://doi.org/10.1016/j.indcrop.2024.119528>

Liao, C., Li, Y., & Tjong, S. C. (2019). Bactericidal and cytotoxic properties of silver nanoparticles. *International Journal of Molecular Sciences*, 20(2), Article 449.
<https://doi.org/10.3390/ijms20020449>

Libanori, A., Chen, G., Zhao, X., Zhou, Y., & Chen, J. (2022). Smart textiles for personalized healthcare. *Nature Electronics*, 5(3), 142-156.
<https://doi.org/10.1038/s41928-022-00723-z>

Maneewattanapinyo, P., Pichayakorn, W., Monton, C., Dangmanee, N., Wunnakup, T., & Suksaeree, J. (2023). Effect of ionic liquid on silver-nanoparticle-complexed *Ganoderma applanatum* and its topical film formulation. *Pharmaceutics*, 15(4), Article 1098.
<https://doi.org/10.3390/pharmaceutics15041098>

Monika, P., Chandraprabha, M. N., Hari Krishna, R., Vittal, M., Likhitha, C., Pooja, N., ... & C, M. (2024). Recent advances in pomegranate peel extract mediated nanoparticles for clinical and biomedical applications. *Biotechnology and*

Genetic Engineering Reviews, 40(4), 3379-3407.
<https://doi.org/10.1080/02648725.2022.2122299>

Neciosup-Puican, A. A., Pérez-Tulich, L., Trujillo, W., & Parada-Quinayá, C. (2024). Green synthesis of silver nanoparticles from anthocyanin extracts of Peruvian purple potato INIA 328 *Kulli Papa*. *Nanomaterials*, 14(13), Article 1147. <https://doi.org/10.3390/nano14131147>

Nie, P., Zhao, Y., & Xu, H. (2023). Synthesis, applications, toxicity and toxicity mechanisms of silver nanoparticles: A review. *Ecotoxicology and Environmental Safety*, 253, Article 114636. <https://doi.org/10.1016/j.ecoenv.2023.114636>

Noga, M., Milan, J., Frydrych, A., & Jurowski, K. (2023). Toxicological aspects, safety assessment, and green toxicology of silver nanoparticles (AgNPs) critical review: State of the art. *International Journal of Molecular Sciences*, 24(6), Article 5133. <https://doi.org/10.3390/ijms24065133>

Rajaboopathi, S., & Thambidurai, S. (2018). Evaluation of UPF and antibacterial activity of cotton fabric coated with colloidal seaweed extract functionalized silver nanoparticles. *Journal of Photochemistry and Photobiology B: Biology*, 183, 75-87. <https://doi.org/10.1016/j.jphotobiol.2018.04.028>

Rehan, M., Elshemy, N. S., Haggag, K., Montaser, A. S., & Ibrahim, G. E. (2020). Phytochemicals and volatile compounds of peanut red skin extract: Simultaneous coloration and in situ synthesis of silver nanoparticles for multifunctional viscose fibers. *Cellulose*, 27(17), 9893-9912. <https://doi.org/10.1007/s10570-020-03452-8>

Rehan, M., Ibrahim, G. E., Mashaly, H. M., Hasanin, M., Rashad, H. G., & Mowafy, S. (2022). Simultaneous dyeing and multifunctional finishing of natural fabrics with Hibiscus flowers extract. *Journal of Cleaner Production*, 374, Article 133992. <https://doi.org/10.1016/j.jclepro.2022.133992>

Rehman, M., Fahad, S., Du, G., Cheng, X., Yang, Y., Tang, K., ... & Deng, G. (2021). Evaluation of hemp (*Cannabis sativa* L.) as an industrial crop: A review. *Environmental Science and Pollution Research*, 28(38), 52832-52843. <https://doi.org/10.1007/s11356-021-16264-5>

Roy, S., & Rhim, J. W. (2021). Anthocyanin food colorant and its application in pH-responsive color change indicator films. *Critical Reviews in Food Science and Nutrition*, 61(14), 2297-2325. <https://doi.org/10.1080/10408398.2020.1776211>

Sadeghi-Kiakhani, M., Tehrani-Bagha, A. R., Safapour, S., Eshaghloo-Galugahi, S., & Etezad, S. M. (2021). Ultrasound-assisted extraction of natural dyes from Hawthorn fruits for dyeing polyamide fabric and study its fastness, antimicrobial, and antioxidant properties. *Environment, Development and Sustainability*, 23(6), 9163-9180. <https://doi.org/10.1007/s10668-020-01017-0>

Sánchez, G. R., Castilla, C. L., Gómez, N. B., García, A., Marcos, R., & Carmona, E. R. (2016). Leaf extract from the endemic plant *Peumus boldus* as an effective bioproduct for the green synthesis of silver nanoparticles. *Materials Letters*, 183, 255-260. <https://doi.org/10.1016/j.matlet.2016.07.115>

Sasunthon, N., Laksee, S., & Pisitsak, P. (2025). Preparation of hemp fabrics with durable UV-protective and antibacterial properties using silver nanoparticles. *Journal of Nanotechnology*, 2025(1), Article 9695944. <https://doi.org/10.1155/jnt/9695944>

Schumacher, A. G. D., Pequito, S., & Pazour, J. (2020). Industrial hemp fiber: A sustainable and economical alternative to cotton. *Journal of Cleaner Production*, 268, Article 122180. <https://doi.org/10.1016/j.jclepro.2020.122180>

Simončič, B., & Klemenčič, D. (2016). Preparation and performance of silver as an antimicrobial agent for textiles: A review. *Textile Research Journal*, 86(2), 210-223. <https://doi.org/10.1177/0040517515586157>

Srisod, S., Motina, K., Inprasit, T., & Pisitsak, P. (2018). A green and facile approach to durable antimicrobial coating of cotton with silver nanoparticles, whey protein, and natural tannin. *Progress in Organic Coatings*, 120, 123-131. <https://doi.org/10.1016/j.porgcoat.2018.03.007>

Suhag, R., Kumar, R., Dhiman, A., Sharma, A., Prabhakar, P. K., Gopalakrishnan, K., ... & Singh, A. (2023). Fruit peel bioactives, valorisation into nanoparticles and potential applications: A review. *Critical Reviews in*

Food Science and Nutrition, 63(24), 6757-6776.
<https://doi.org/10.1080/10408398.2022.2043237>

Tat, T., Chen, G., Zhao, X., Zhou, Y., Xu, J., & Chen, J. (2022). Smart textiles for healthcare and sustainability. *ACS Nano*, 16(9), 13301-13313.
<https://doi.org/10.1021/acsnano.2c06287>

Vasyliev, G., & Vorobyova, V. (2020). Valorization of food waste to produce eco-friendly means of corrosion protection and “green” synthesis of nanoparticles. *Advances in Materials Science and Engineering*, 2020(1), Article 6615118.
<https://doi.org/10.1155/2020/6615118>

Velmurugan, P., Kim, J. I., Kim, K., Park, J. H., Lee, K. J., Chang, W. S., ... & Oh, B. T. (2017). Extraction of natural colorant from purple sweet potato and dyeing of fabrics with silver nanoparticles for augmented antibacterial activity against skin pathogens. *Journal of Photochemistry and Photobiology B: Biology*, 173, 571-579.
<https://doi.org/10.1016/j.jphotobiol.2017.07.001>

Yin, Y., Jia, J., Wang, T., & Wang, C. (2017). Optimization of natural anthocyanin efficient extracting from purple sweet potato for silk fabric dyeing. *Journal of Cleaner Production*, 149, 673-679.
<https://doi.org/10.1016/j.jclepro.2017.02.134>

Yu, Z., He, H., Liu, J., Li, Y., Lin, X., Zhang, C., & Li, M. (2020). Simultaneous dyeing and deposition of silver nanoparticles on cotton fabric through in situ green synthesis with black rice extract. *Cellulose*, 27(3), 1829-1843.
<https://doi.org/10.1007/s10570-019-02910-2>

Yu, Z., Liu, J., He, H., Wang, Y., Zhao, Y., Lu, Q., ... & Peng, Y. (2021). Green synthesis of silver nanoparticles with black rice (*Oryza sativa* L.) extract endowing carboxymethyl chitosan modified cotton with high anti-microbial and durable properties. *Cellulose*, 28(3), 1827-1842.
<https://doi.org/10.1007/s10570-020-03639-z>